Supporting Information

Elegant Z-scheme-Dictated g-C_3N_4 Enwrapped WO_3 Superstructures: A Multifarious Platform for Versatile Photoredox Catalysis

Zhi-Yu Liang [a,b], Jin-Xin Wei [a,b], Xiu Wang [a,b], Yan Yu [a,b,*], Fang-Xing Xiao [a*]

[a]College of Materials Science and Engineering, Fuzhou University, New Campus, Minhou, Fujian Province 350108, China

[b]Key Laboratory of Eco-materials Advanced Technology (Fuzhou University), Fujian Province University, China

*Corresponding author. Fax: +86 591 22866534;

E-mail address: yuyan@fzu.edu.cn
fxxiao@fzu.edu.cn

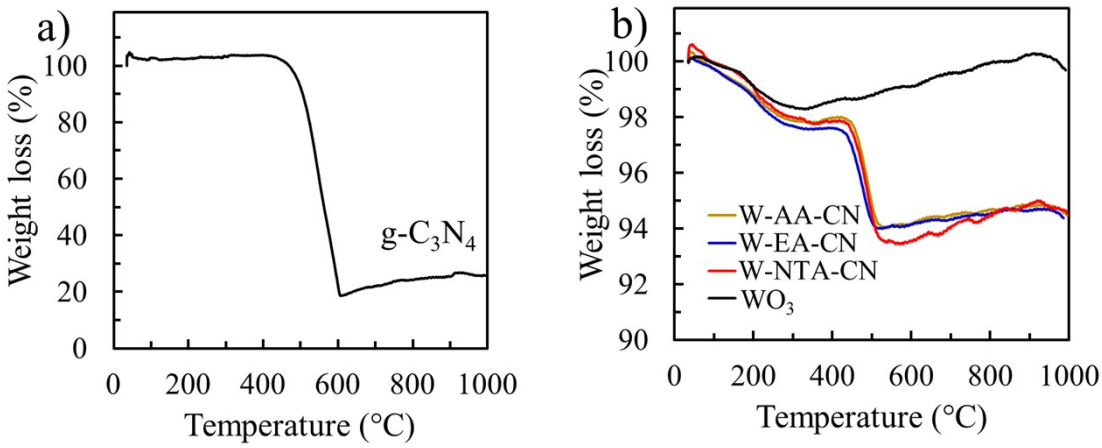

Fig. S1. TGA results of (a) g-C_3N_4 and (b) W-AA-CN, W-EA-CN, W-NTA-CN, WO_3.

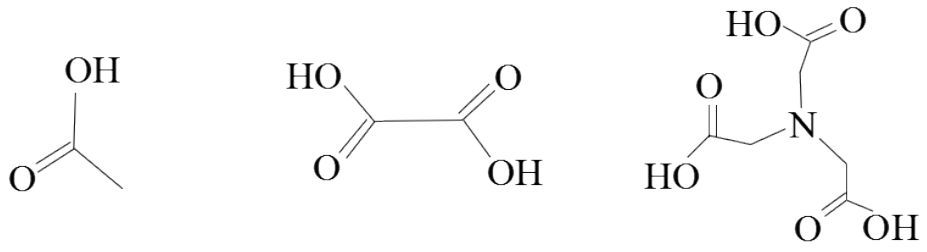

acetic acid ethanedioic acid nitrilotriacetic acid

Fig. S2. Molecular structures of acetic acid (AA), ethanedioic acid (EA) and nitrilotriacetic acid (NTA) used for the synthesis of different WO_3 superstructures.

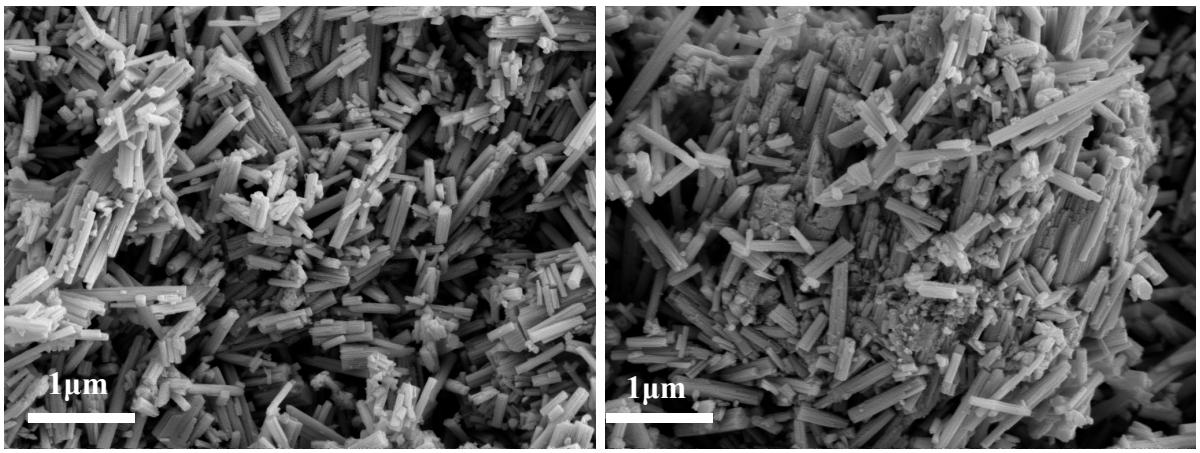

Fig. S3. FESEM images of WO_3 prepared without using organic acids.

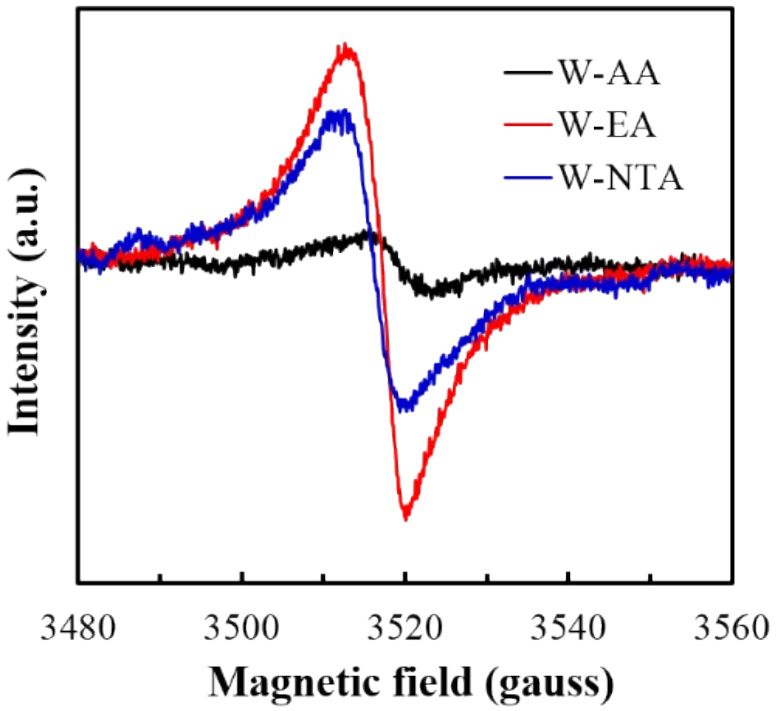

Fig. S4. ESR spectra of oxygen vacancy for W-AA, W-EA and W-NTA.

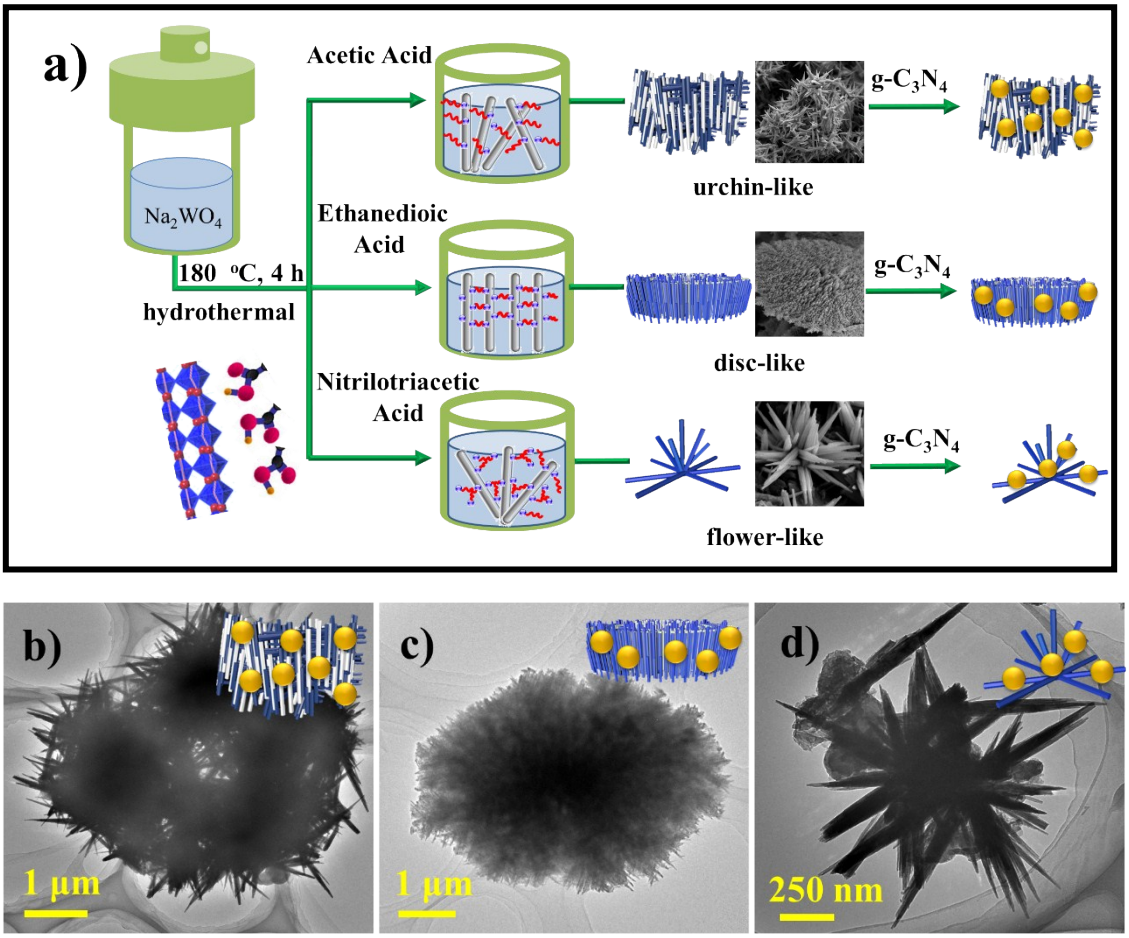

Fig. S5. (a) Possible growth mechanism of WO_3 superstructures induced by organic acids. TEM images of (b) W-AA-CN, (c) W-EA-CN and (d) W-NTA-CN heterostructures.

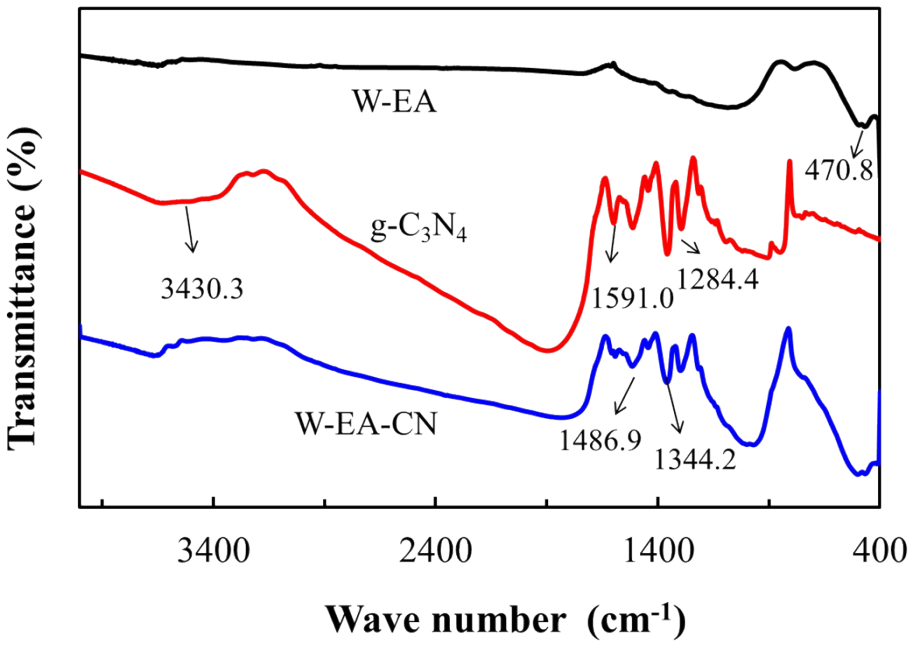

Fig. S6. FTIR spectra of W-EA, g-C_3N_4, and W-EA-CN.

Note： **Fig. S6** shows the FTIR spectra of W-EA, g-C_3N_4 and W-EA-CN. The FTIR spectra of W-EA and W-EA-CN illustrate the characteristic absorption bands at 450–760cm^{-1}, which are attributed to the W-O stretching and W-O-W bridging stretching modes[1, 2]. FTIR spectrum of g-C_3N_4 is featured by the presence of several peaks located between 1200 and 1650 cm^{-1}, which can be assigned to the stretching vibration mode of aromatic C-N heterocycles containing either trigonal N(-C)$_3$ or bridging C-NH-C units, indicating the formation of C-N-C bonds [3, 4]. Additionally, a broad band at around 3430 cm^{-1} was clearly seen in the FTIR spectrum of g-C_3N_4, indicative of the stretching vibration mode of N-H groups [5, 6]. Noteworthily, all characteristic peaks of g-C_3N_4 can be clearly observed in the FTIR spectrum of W-EA-CN, verifying successful attachment of g-C_3N_4 on the WO_3 framework.

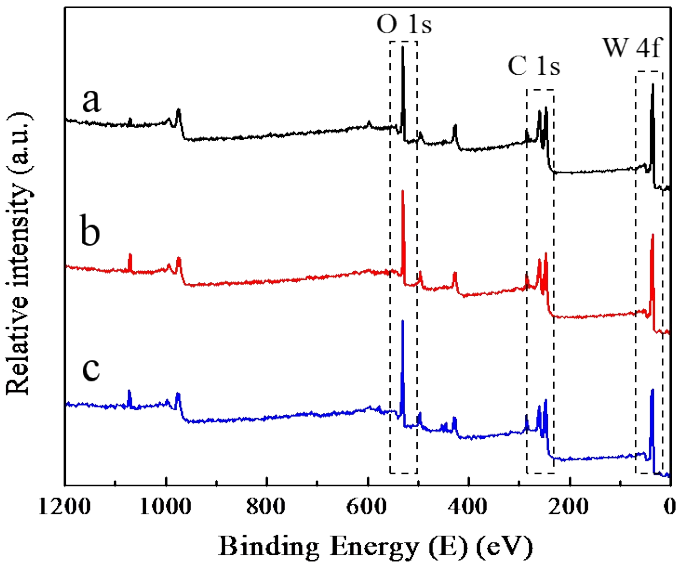

Fig. S7. Survey XPS spectra of (a) W-AA, (b) W-EA and (c) W-NTA.

Tab. S1. E_g, E_{CB} and E_{VB} of WO_3 and g-C_3N_4 in blank sample and heterostructures.

	E_g /eV	E_{VB} /eV	E_{CB} /eV
W-AA	2.75	+3.37	+0.62
W-EA	2.56	+3.27	+0.71
W-NTA	2.67	+3.33	+0.66
g-C_3N_4	2.68	+1.57	−1.11
W-AA-CN	2.70	–	–
W-EA-CN	2.61	–	–
W-NTA-CN	2.66	–	–

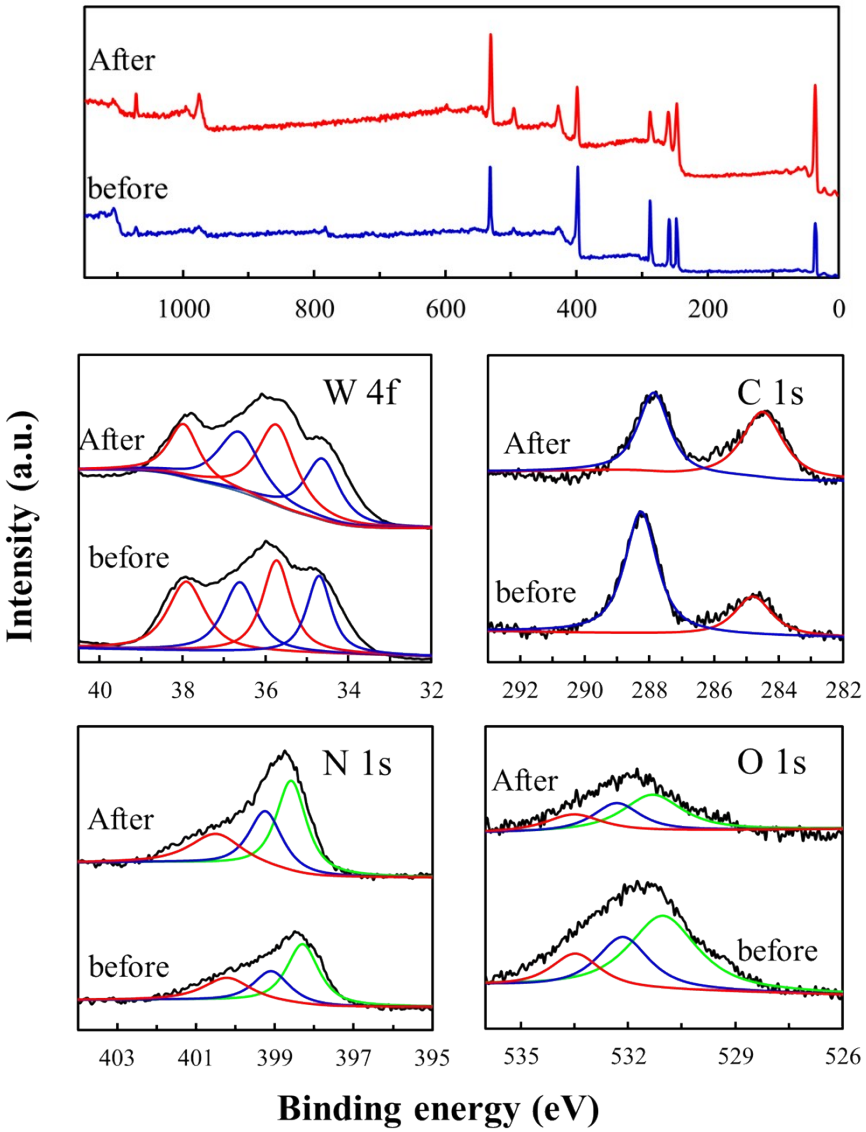

Fig. S8. Survey and high-resolution XPS spectra of W-EA-CN heterostructure before and after five successive cyclic photocatalytic reactions.

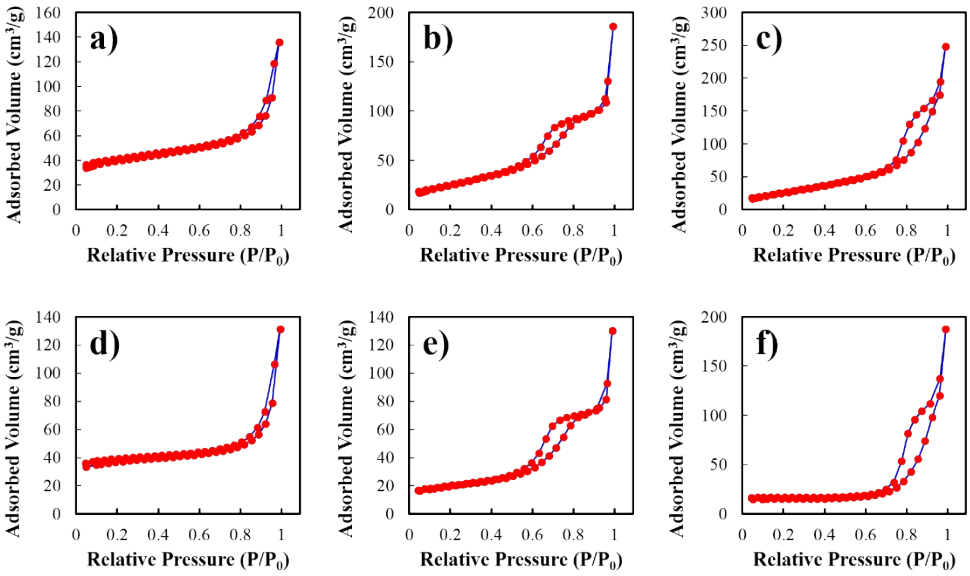

Fig. S9. Specific surface areas of (a) W-AA, (b) W-EA, (c) W-NTA, (d) W-AA-CN, (e) W-EA-CN and (f) W-NTA-CN heterostructures.

Tab. S2. Specific surface area, pore volume and pore size of different samples.

	BET surface area (m^2/g)	**Pore volume** (cm^3/g)	**Pore size** (nm)
W-AA	97.5	0.385	6.2
W-AA-CN	44.2	0.291	10.3
W-EA	128.9	0.200	5.3
W-EA-CN	65.6	0.175	8.4
W-NTA	167.6	0.488	10.4
W-NTA-CN	112.7	0.154	11.2

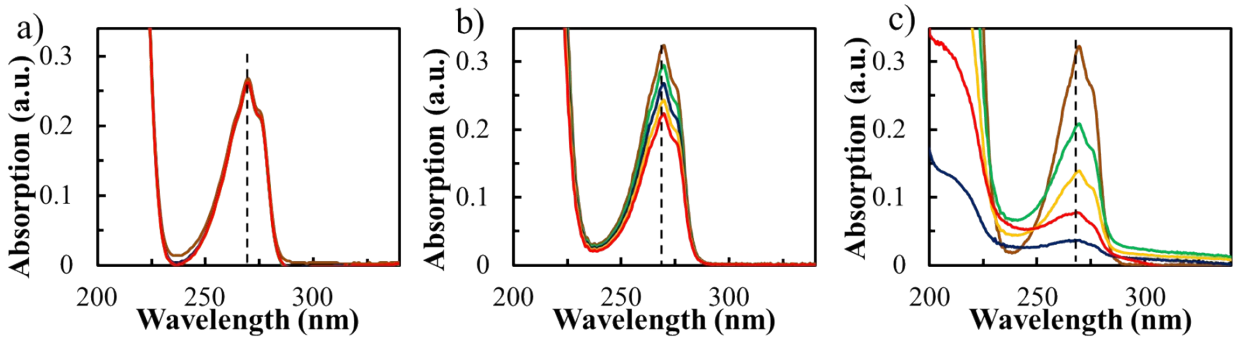

Fig. S10. UV-vis spectra of phenol (270 nm) degraded by (a) W-EA, (b) g-C_3N_4 and W-EA-CN.

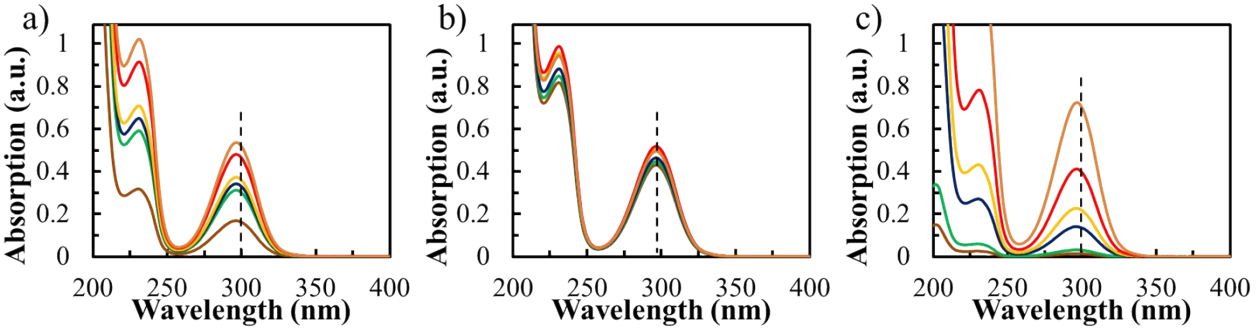

Fig. S11. UV-vis spectra of salicylic acid (300 nm) degraded by (a) W-EA, (b) g-C_3N_4 and W-EA-CN.

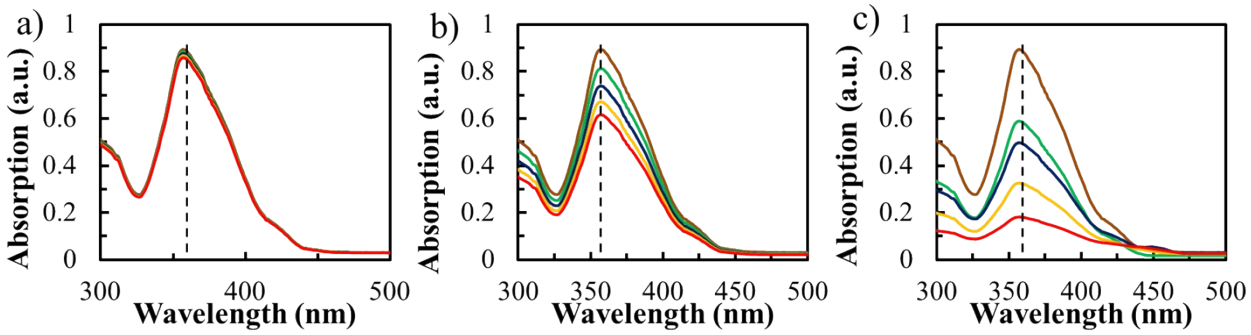

Fig. S12. UV-vis spectra of Cr(VI) (364 nm) degraded by (a) W-EA, (b) g-C_3N_4 and W-EA-CN.

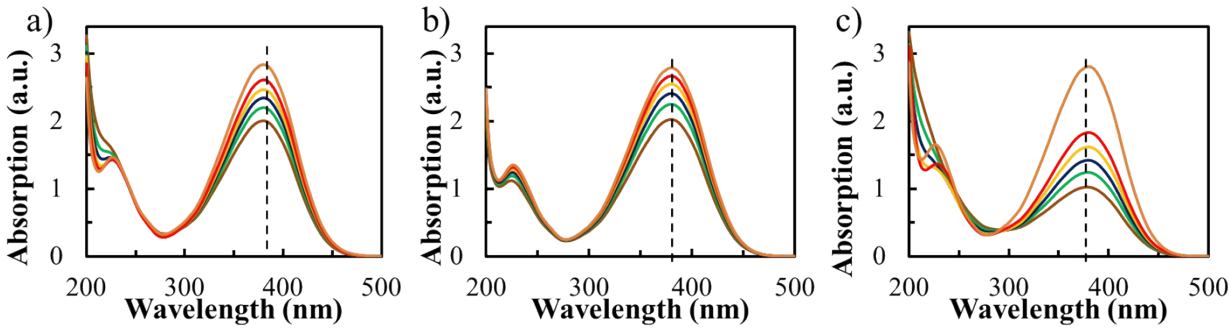

Fig. S13. UV-vis spectra of 4-nitroaniline (380 nm) degraded by (a) W-EA, (b) g-C_3N_4 and W-EA-CN.

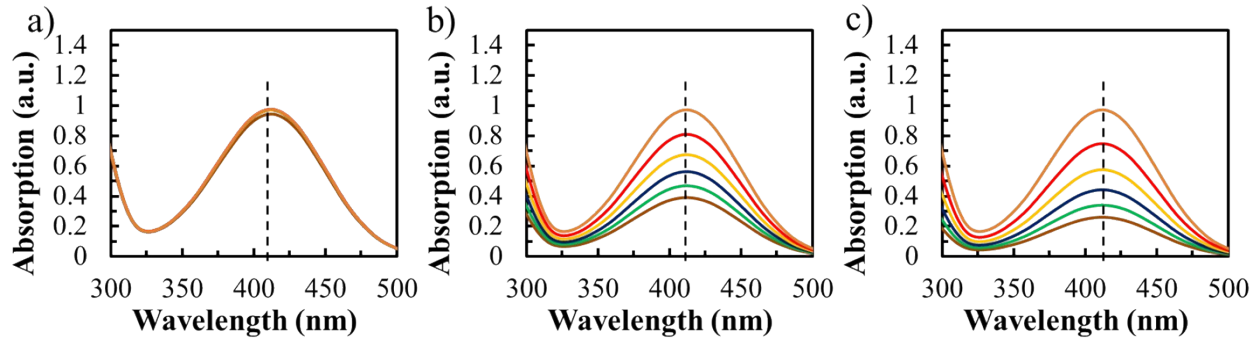

Fig. S14. UV-vis spectra of 2-nitroaniline (412 nm) degraded by (a) W-EA, (b) g-C_3N_4 and W-EA-CN.

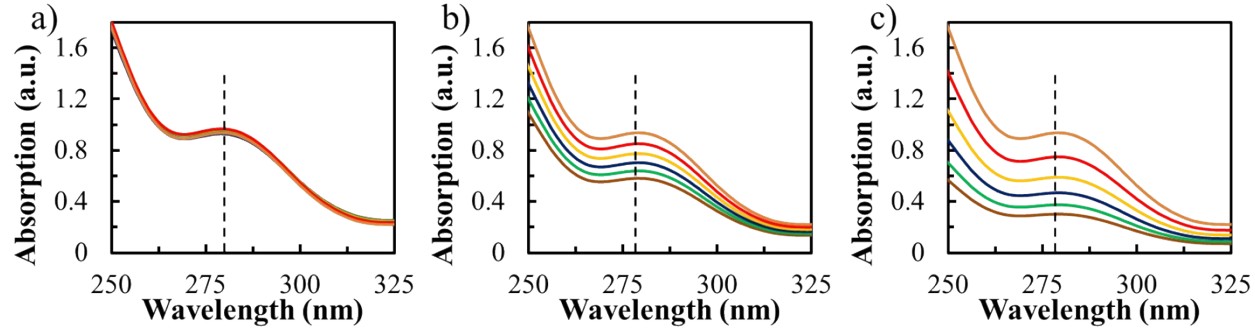

Fig. S15. UV-vis spectra of 3-nitroaniline (279 nm) degraded by (a) W-EA, (b) g-C_3N_4 and W-EA-CN.

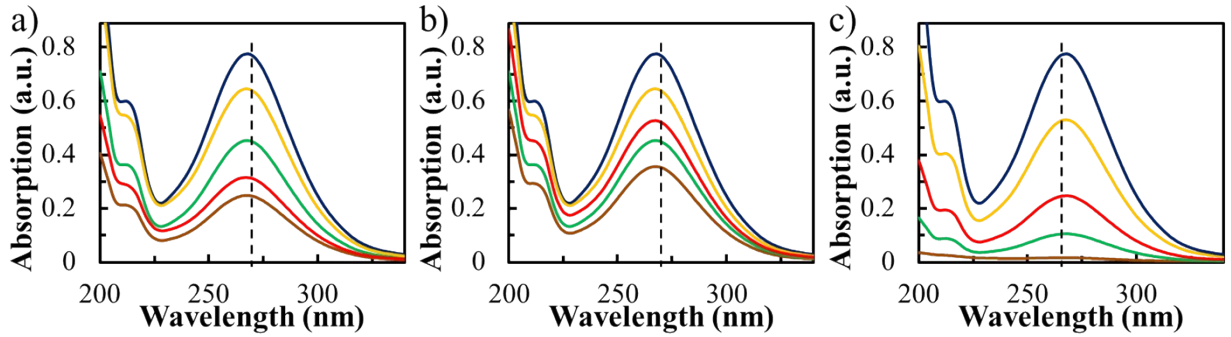

Fig. S16. UV-vis spectra of nitrobenzene (268 nm) degraded by (a) W-EA, (b) g-C_3N_4 and W-EA-CN.

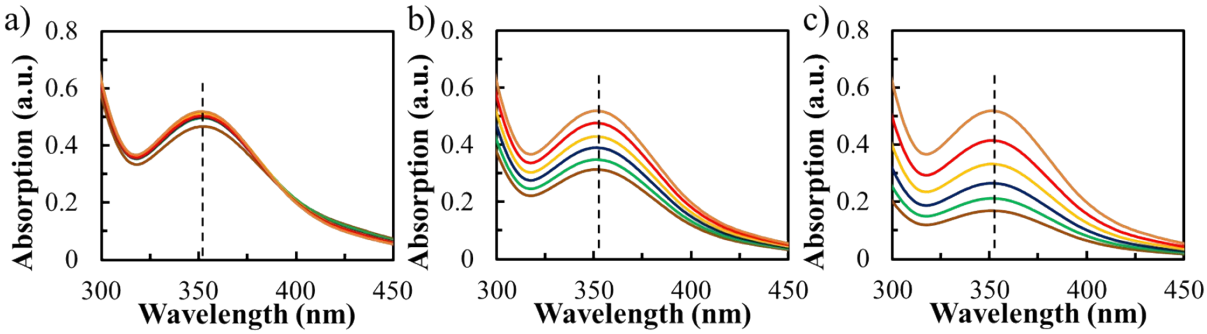

Fig. S17. UV-vis spectra of 2-nitrophenol (352 nm) degraded by (a) W-EA, (b) g-C_3N_4 and W-EA-CN.

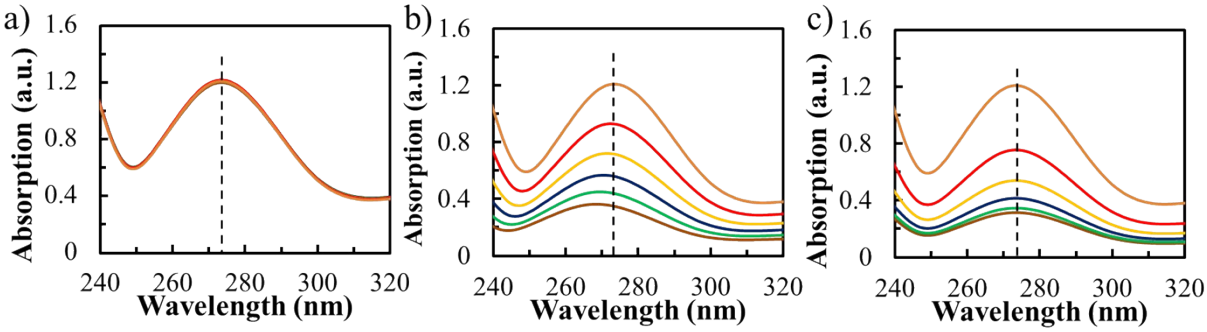

Fig. S18. UV-vis spectra of 3-nitrophenol (272 nm) degraded by (a) W-EA, (b) g-C_3N_4 and W-EA-CN.

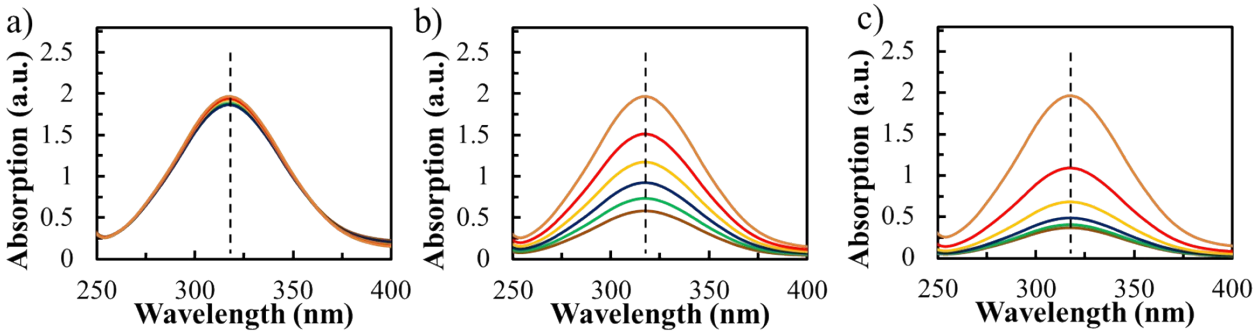

Fig. S19. UV-vis spectra of 4-nitrophenol (317 nm) degraded by (a) W-EA, (b) g-C_3N_4 and W-EA-CN.

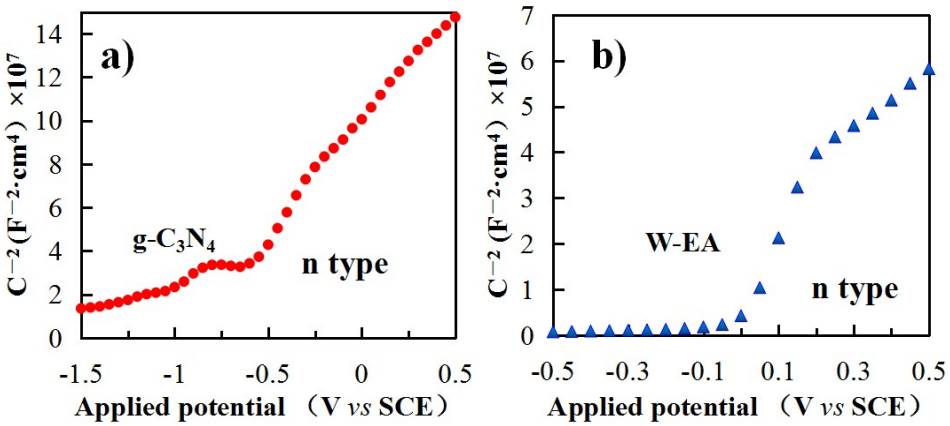

Fig. S20. Mott−Schottky results of (a) g-C_3N_4 and (b) W-EA.

Appendix: bandgap energy calculation

The bandgap energy of the photocatalysts is calculated based on the following equations [7, 8]:

$$\alpha h\nu = A(h\nu - E_g)^{n/2} \quad (1)$$

where h, v, A, and E_g are absorption coefficient, Planck constant, light frequency, proportionality and bandgap energy, respectively.

The band edge positions of CB and VB for semiconductors can be determined by the following equations:

$$E_{VB} = X - E_e + 0.5E_g \quad (2)$$

$$E_{CB} = E_{VB} - E_g \quad (3)$$

where X is the absolute electronegativity of the semiconductor, X are 4.73 and 6.49 eV for g-C_3N_4 and WO_3 and E_e is the energy of free electrons on the hydrogen scale (ca. 4.5 eV).

References

1. K. Katsumata, R. Motoyoshi, N. Matsushita and K. Okada, *J. Hazard. Mater.*, 2013, **260**, 475-482.
2. J. Li, H. Hao and Z. Zhu, *Mater. Lett.*, 2016, **168**, 180-183.
3. Z. W. Zhao, Y. J. Sun and F. Dong, *Nanoscale*, 2015, **7**, 15-37.
4. Y. Zheng, L. H. Lin, B. Wang and X. C. Wang, *Angew. Chem. Int. Ed.*, 2015, **54**, 12868-12884.
5. S. W. Cao, J. X. Low, J. G. Yu and M. Jaroniec, *Adv. Mater.*, 2015, **27**, 2150-2176.
6. J. J. Zhu, P. Xiao, H. L. Li and S. A. C. Carabineiro, *Acs Appl. Mater. Interfaces*, 2014, **6**, 16449-16465.
7. S.F. Chen, Y.F. Hu, S.G. Meng, X.L. Fu, Appl. Catal. B-Environ., 2014, **150,** 564-573.
8. H.F. Li, H.T. Yu, X. Quan, S. Chen, Y.B. Zhang, *Acs Appl. Mater. Interfaces*, 2016, **8**,2111-2119.